PERGAMON

Journal of Structural Geology 24 (2002) 435–449

JOURNAL OF STRUCTURAL GEOLOGY

www.elsevier.com/locate/jstrugeo

The origin and evolution of complex transfer zones (graben shifts) in conjugate fault systems around the Funan Field, Pattani Basin, Gulf of Thailand

A. Kornsawan[a], C.K. Morley[b,*]

[a]*Unocal Thailand, Ltd, SCB Park Plaza Tower III, 19 Ratchadapisek Road, Chatuchak, Bangkok 10900, Thailand*
[b]*Department of Petroleum Geoscience, University of Brunei Darussalam, Bandar Seri Begawan, 2028, Negara Brunei Darussalam, Brunei*

Received 26 June 2001; accepted 28 June 2001

Abstract

Changes in dip province associated with conjugate fault sets produce complex transfer zones (locally known as graben shifts) between sets of convergent conjugate faults in the Pattani Basin. 3D seismic data over a well-developed graben shift geometry in the Funan Field area of the Pattani Basin has revealed details of the transfer zone development. In map view, the graben shift is seen as west dipping faults forming a wedge-shaped incursion into a zone of east-dipping faults. The wedge boundaries trend NE–SW and NW–SE at a high angle to the N–S striking normal faults. Within the transfer zones, faults only slightly overlap with their neighbours, with individual faults tending to widen upwards. The narrow regions of overlap indicate displacement transfer must occur between more widely separated faults, not neighbouring faults. The initial Oligocene–Early Miocene syn-rift fault pattern appears to have been strongly influenced by pre-existing basement trends as indicated by: (1) the restriction of west dipping secondary faults to the present day area of the graben shift, (2) the line of the NE–SW boundary to the graben shift coinciding with fault segment linkage geometries in two major syn-rift faults, and (3) curvature of minor fault tips into the transfer zone. The subsequent conjugate fault system developed during thermal subsidence shows that the dip asymmetry and map-boundaries of the fault dip panels are strongly influenced by the syn-rift fault geometry. There is no indication of active strike-slip faulting affecting the graben shift geometry. Fault displacement diagrams commonly show linkage between deeper and shallower displacement maxima, indicating early (Late Oligocene–Early Miocene), minor, west-dipping normal faults influenced the location and width of higher Middle–Late Miocene conjugate faults. Hence, two stages of structural inheritance led to the Middle–Late Miocene graben shift geometry. © 2002 Elsevier Science Ltd. All rights reserved.

Keywords: Complex transfer zones; Graben shifts; Conjugate fault systems; Gulf of Thailand; Pattani basin

1. Introduction

The Pattani Basin lies offshore in the Gulf of Thailand (Fig. 1) and is the most productive basin for hydrocarbons in Thailand (e.g. Bustin and Chonchawalit, 1995; Jardine, 1997). In the literature it is described as having an Oligocene–Middle Miocene syn-rift section and a Middle Miocene–Recent sag basin sequence (Jardine, 1997; Fig. 2). However the Pattani Basin does not resemble a typical rift-sag sequence. Regionally the syn-rift section does not display the large half grabens typical of rift sequences in general, or those more specifically observed in the Oligo–Miocene Kra and Western Basins, which lie west of the Pattani Basin (Watcharanantakul and Morley, 2000; Fig. 1). The syn-rift section in the Pattani Basin tends to be bounded by relatively small displacement faults (Figs. 1 and 2). However, more locally on 3D seismic reflection data it is possible to distinguish relatively large displacement (1000 + m) normal faults, associated with small half grabens in the Oligocene–Middle Miocene sequences from overlying relatively small displacement (typically 200–300 m), conjugate normal fault systems that affect the post-rift section (Fig. 2). Structural traps in the Pattani Basin are unusual for rift-sag sequences; the large fields are associated with broad antiformal structures formed within the grabens of converging conjugate normal fault systems in the post-rift section (Fig. 2). It is these conjugate normal fault systems around the Funan field which are the focus of this study.

The Funan C platform area is bound to the northwest and southeast by abrupt changes in the dominant dip direction of groups or domains of normal faults that form conjugate fault

---

* Corresponding author.
E-mail address: chrismmorley@hotmail.com (C.K. Morley).

0191-8141/02/$ - see front matter © 2002 Elsevier Science Ltd. All rights reserved.
PII: S0191-8141(01)00080-3

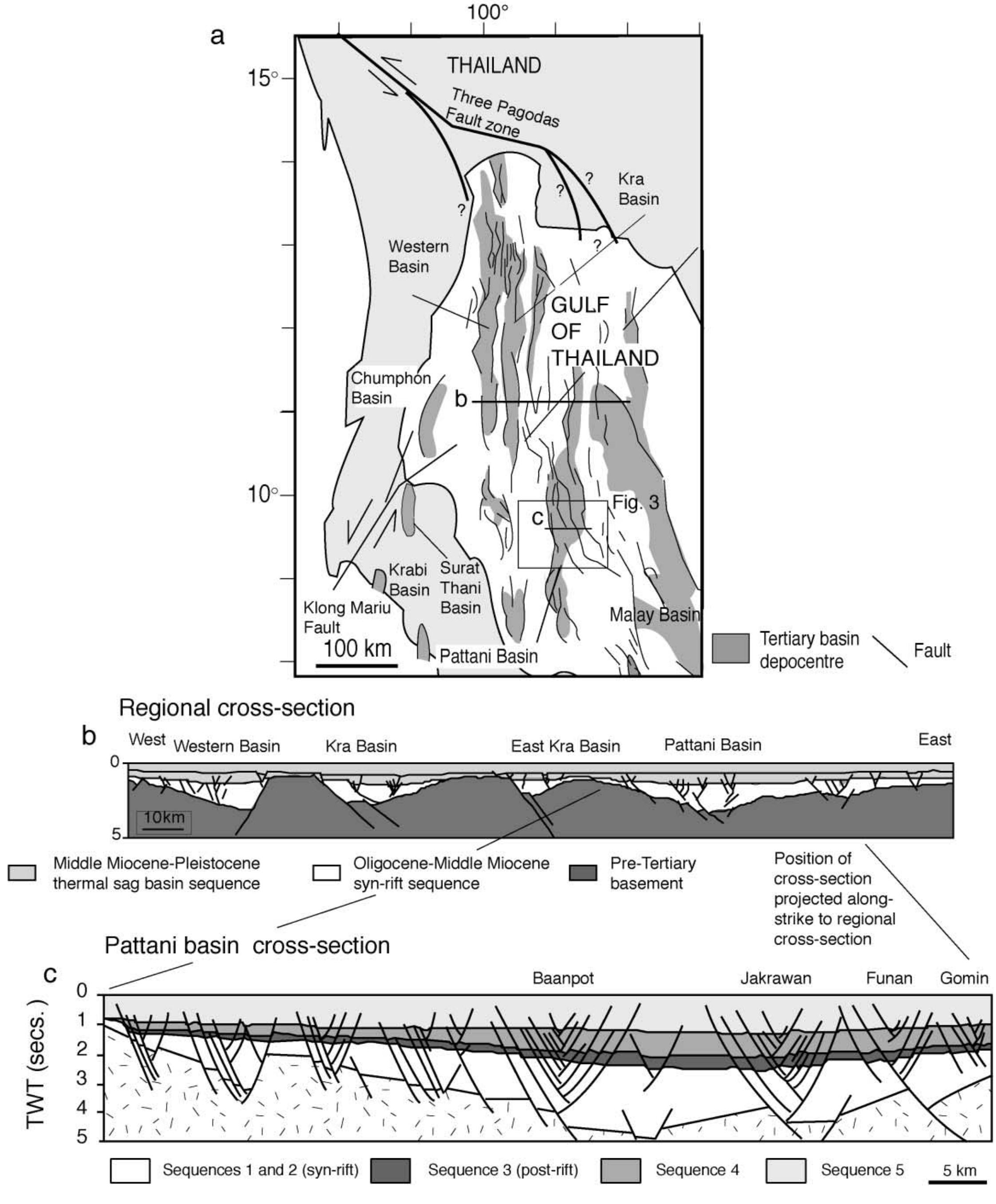

Fig. 1. (a) Location map for Tertiary basins in the Gulf of Thailand (modified from Polachan and Sattayarak, 1989). (b) Cross-section through the northern Gulf of Thailand (from Oudom-Ugsorn et al., 1986). (c) Cross-section through Pattani Basin (from Watcharanantakul and Morley, 2000). The relative position of cross-section c to cross-section b is indicated; however it should be noted that the actual location of section c is south of section b.

systems (Fig. 3). Such changes in dip domain are a common feature in the Pattani Basin and are informally known as '*graben shifts*'. They are complex transfer zones between arrays of downward-converging conjugate faults that give rise to areas of antiformal strata dip. In the study area the graben shifts separate relatively steep west-dipping strata (6–8°W) from the flatter reflections (2–4°E) of the Funan east flank, creating a re-entrant of the east flank into the west flank. Using 3D seismic data, fault patterns can be identified with a high degree of confidence. This study investigates the origin of the graben shift geometries using 3D seismic data.

There is little discussion of the origins of the graben shift geometries in the Pattani Basin, in the literature, but within oil companies exploring the basin several possible influences have been discussed including: (1) the effects of pre-existing fabrics in pre-Tertiary 'basement' on a simple extensional fault system, (2) active strike-slip faulting

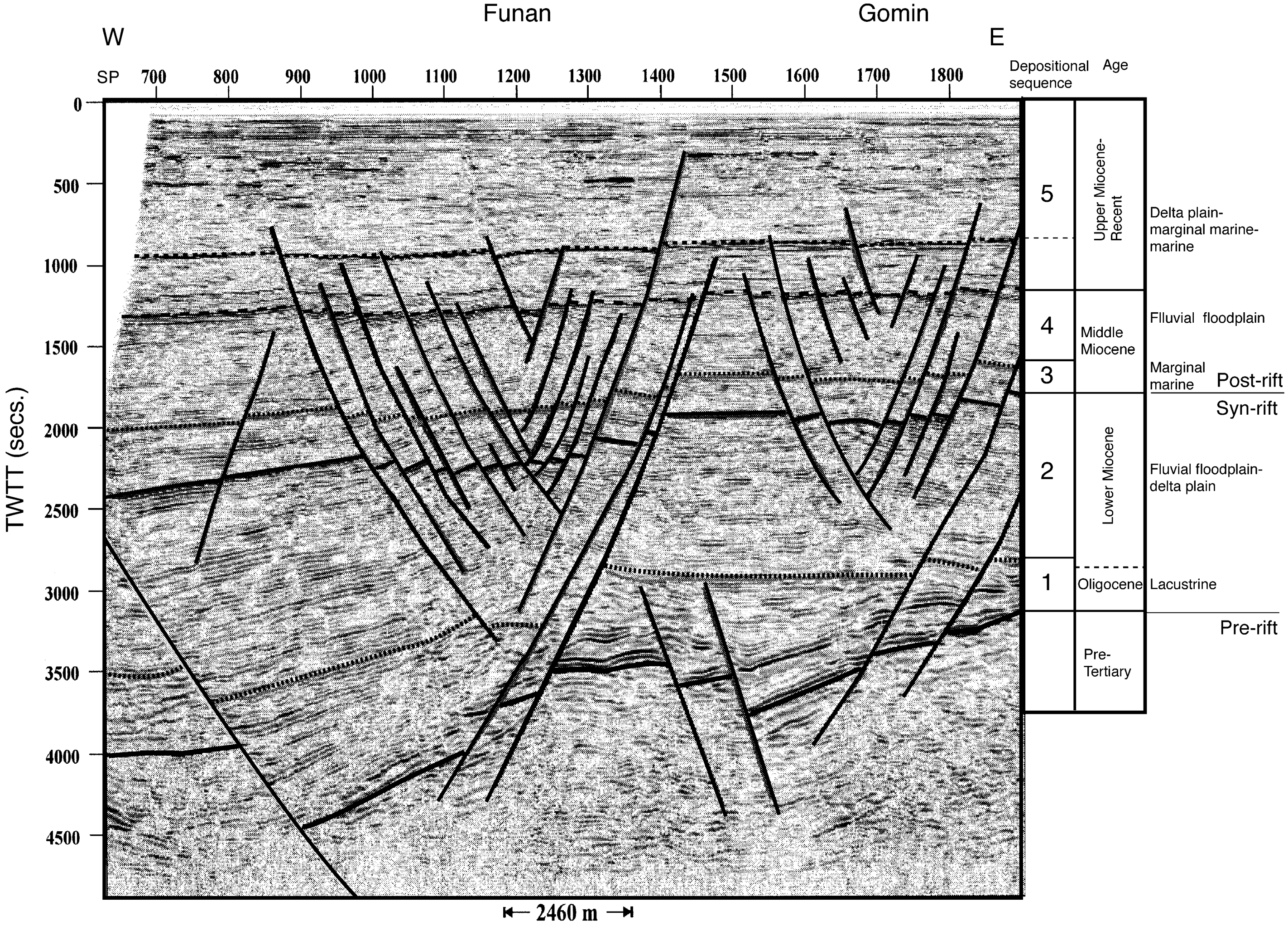

Fig. 2. Example of 3D seismic reflection data across the Funan Field area, with stratigraphic summary based on Jardine (1997). See Fig. 5 for location.

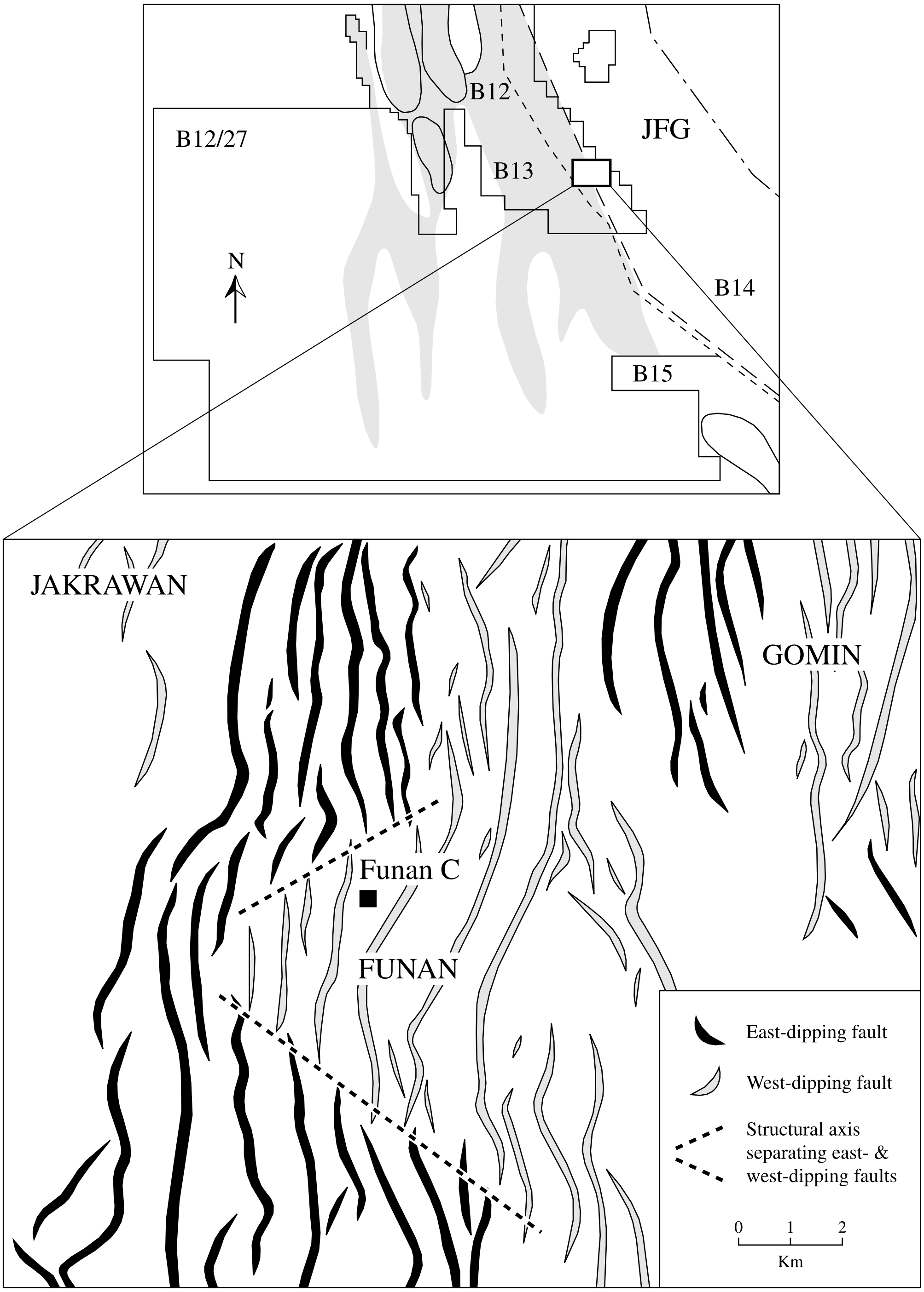

Fig. 3. Map of the graben shift pattern from a horizon within Sequence 3 in the Funan Field area. A salient of west-dipping faults (grey) extends westwards into the province dominated by east-dipping faults (black). See Fig. 1 for location.

interfering with the extensional fault system, and (3) structural development of the post-rift section independent of syn-rift and basement influence. Strike-slip faulting is commonly invoked as a possible explanation for a variety of structural features in the Gulf of Thailand. This is related to the frequently cited Himalayan escape tectonics model (Tapponnier et al., 1982, 1986), where large strike-slip faults caused Tertiary deposition in pull-apart basins (Tapponnier et al., 1986; Polachan and Sattayarak, 1989; Hall, 1996). However, there is considerable divergence of opinion in the literature as to the importance of strike-slip faulting and whether the rift basins opened up as pull-apart basins or independently as extensional basins (e.g. McCabe et al., 1993; Morley et al., 2000; Watcharanantakul and Morley, 2000). Most interpretations of strike-slip faulting have been conducted on the basis of regional features, with

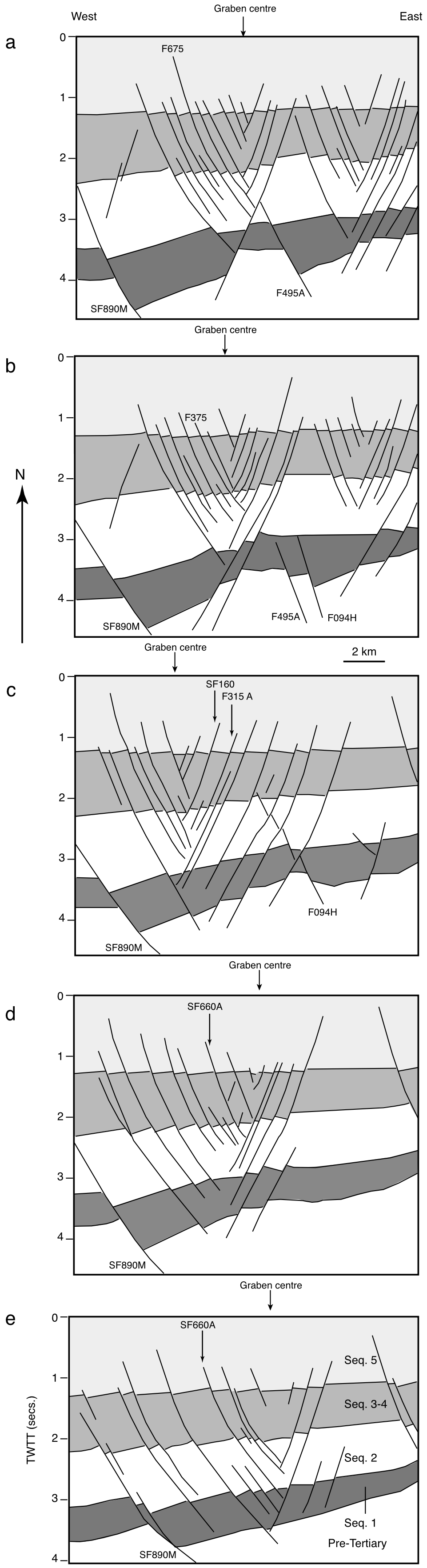

Fig. 4. Cross-sections across the Funan graben shift, illustrating N–S changes in structural style associated with the graben shift. See Fig. 5 for location.

little accompanying detailed analysis. It is the detailed examination of structural features, such as the graben shifts, which will help clarify the role played by strike-slip faulting in the late Tertiary structural evolution of the Gulf of Thailand.

To tackle the problem of understanding the cause of graben shifts using the 3D seismic reflection data (which is the only available data) has obvious problems. In particular, the nature of structural fabrics in basement rocks is not known. However, by examining the fault geometries in as much detail as possible a picture of how the faults developed was built up, which could at least partly answer the questions above. The fault characteristics used include fault displacement maps, fault height–width relationships, isochrons (used here in the sense of contours of equal time difference), time structure contour maps, and fault-plane structure contours.

Vintage marine 3D seismic reflection data from 1987, acquired by Unocal, Thailand, formed the basis for this study. The data contained 400 inlines and 2000 crosslines with spacing of 50 m between the lines. These data cover approximately 720 km^2 of the Funan Field. Interpretation of the seismic data was concentrated on the region where the graben shift occurs, between inlines 550–860 and crosslines 630–1900.

2. Stratigraphy of the Pattani Basin

There are several variations on the stratigraphic scheme for the Pattani Basin (Lian and Bradley, 1986; Pradidtan and Dook, 1992; Jardine, 1997). In this study the stratigraphic section of Unocal is used (Jardine, 1997). The Tertiary section of the Pattani Basin can be divided into five major sequence packages, which reflect low-order relative sea-level changes in the Neogene (Fig. 2). There are two periods of non-deposition around 25 and 10 Ma represented by the Mid-Tertiary Unconformity (MTU) and the Mid-Miocene Unconformity (MMU), respectively.

The structural–stratigraphic evolution of the Pattani Basin as summarised by Jardine (1997) is as follows (Fig. 2): (1) Basin deposition began with initially localised lacustrine and alluvial deposition in the Oligocene (Sequence 1). These are syn-rift deposits. (2) Mostly fluvial and alluvial syn-rift sediments were deposited in the Early Miocene (Sequence 2). (3) Transgressive fluvial and marginal marine deposition occurred in the early Middle Miocene (Sequence 3). Sequence 3 marks the start of post-rift thermal subsidence. (4) Overall regressive fluvial and alluvial deposition occurred in the late Middle Miocene (Sequence 4). (5) Predominantly transgressive marginal

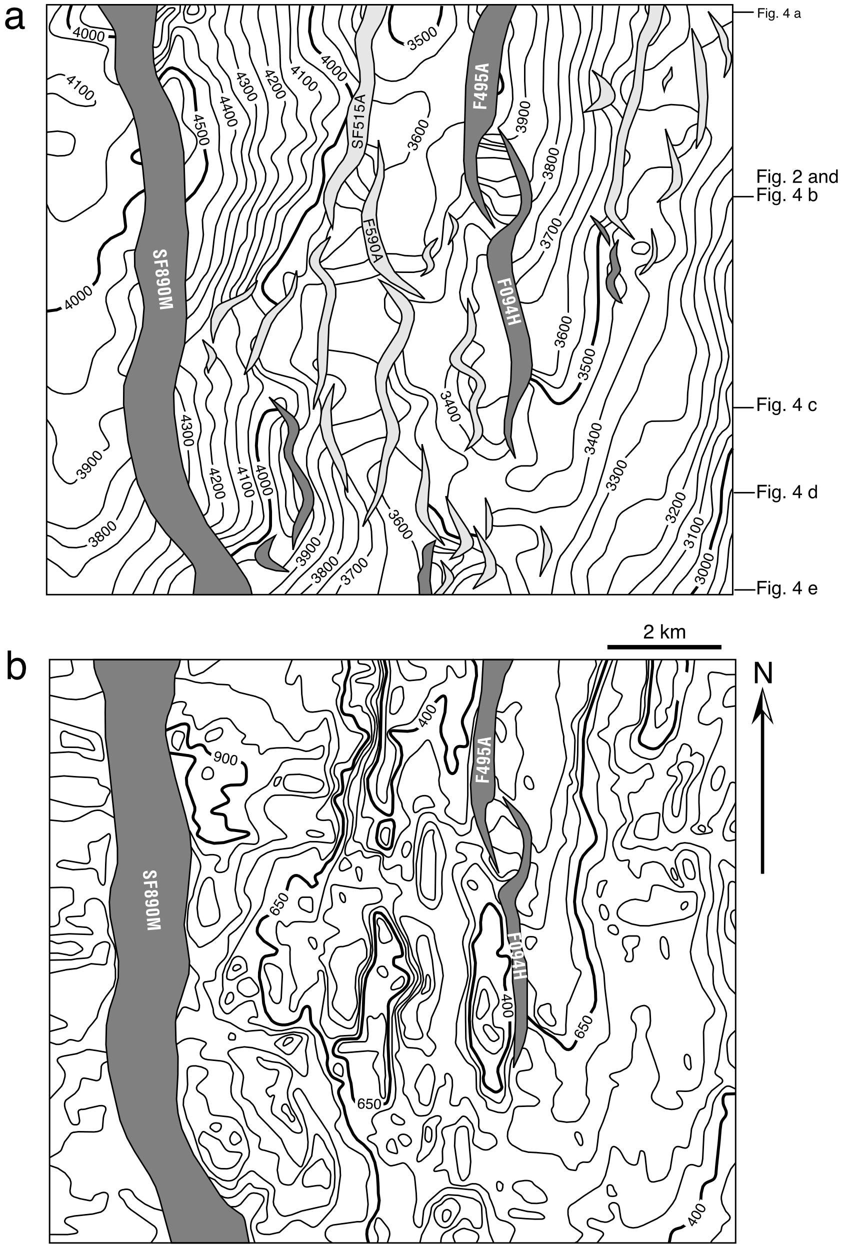

Fig. 5. Time-structure top Sequence 1 (a) and isochron (b) map for Sequence 1. See Fig. 3 for location. East dipping faults are black, west dipping faults are grey. Contours in milliseconds.

marine deposition is characteristic of the Late Miocene–Recent (Sequence 5).

3. Structural geometry of the Funan Field

The post-rift section of the Funan Field is affected by numerous minor conjugate faults. The resulting geometry is a highly faulted north–south trending antiformal structure, 25 km long and 4–8 km wide (Figs. 3 and 4). Fault blocks are 0.5–1 km wide, with structural dips of 2–4° E on the eastern flank, and 6–8° on the western flank. Nearly all hydrocarbon production is from Early–Middle Miocene reservoirs on the eastern flank. A slight isochron thickening, and structural low or 'graben centre' runs along the region that separates the eastern and western flanks of the structure. In the vicinity of the Funan C platform, west-dipping faults on the eastern flank make a prominent wedge-shaped incursion into the east-dipping fault zone. The dip province boundary is abrupt, the northern boundary of the wedge trends NE–SW and the southern boundary trends NW–SE.

On a series of east–west oriented seismic lines passing from south to north, the change in conjugate fault geometry is manifest by a progressive change from dominance of east-dipping faults (Fig. 4a and b) to west-dipping faults (Fig. 4c) then back to east-dipping faults (Fig. 4d and e). This is a

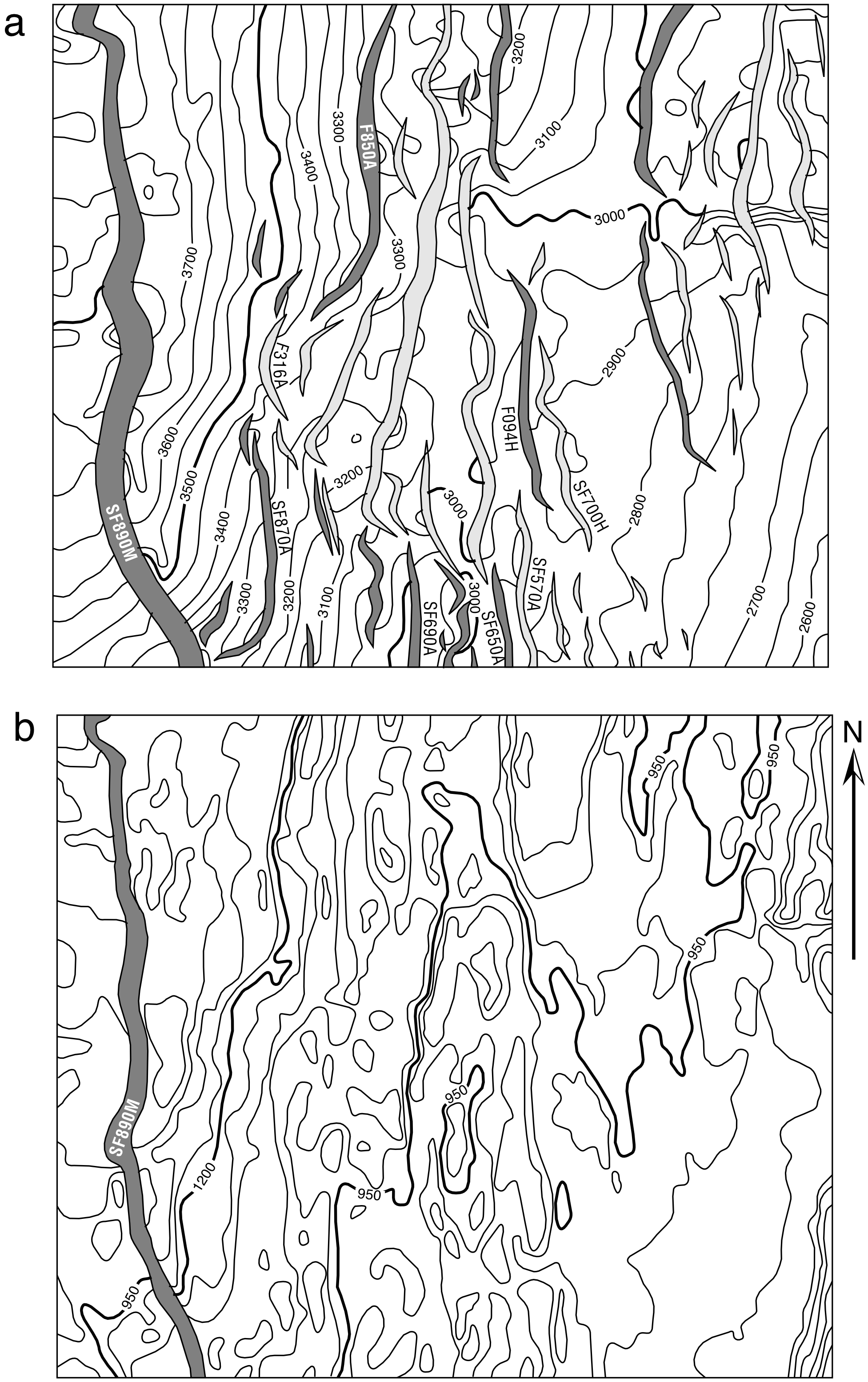

Fig. 6. Time-structure top Sequence 2 (a) and isochron (b) maps for Sequence 2. See Fig. 3 for location. East dipping faults are black, west dipping faults are grey. Contours in milliseconds.

typical pattern for conjugate fault development (e.g. Nicol et al., 1996). The more external conjugate faults pass into pre-Tertiary ‘basement’, but others, closer to the graben centre do not (Figs. 2 and 4). Instead, the faults terminate downwards at east-dipping faults. The faults were mapped to determine the nature of the conjugate fault intersections. In most examples the conjugate faults did not appear to intersect, but instead died out or stopped at a locally

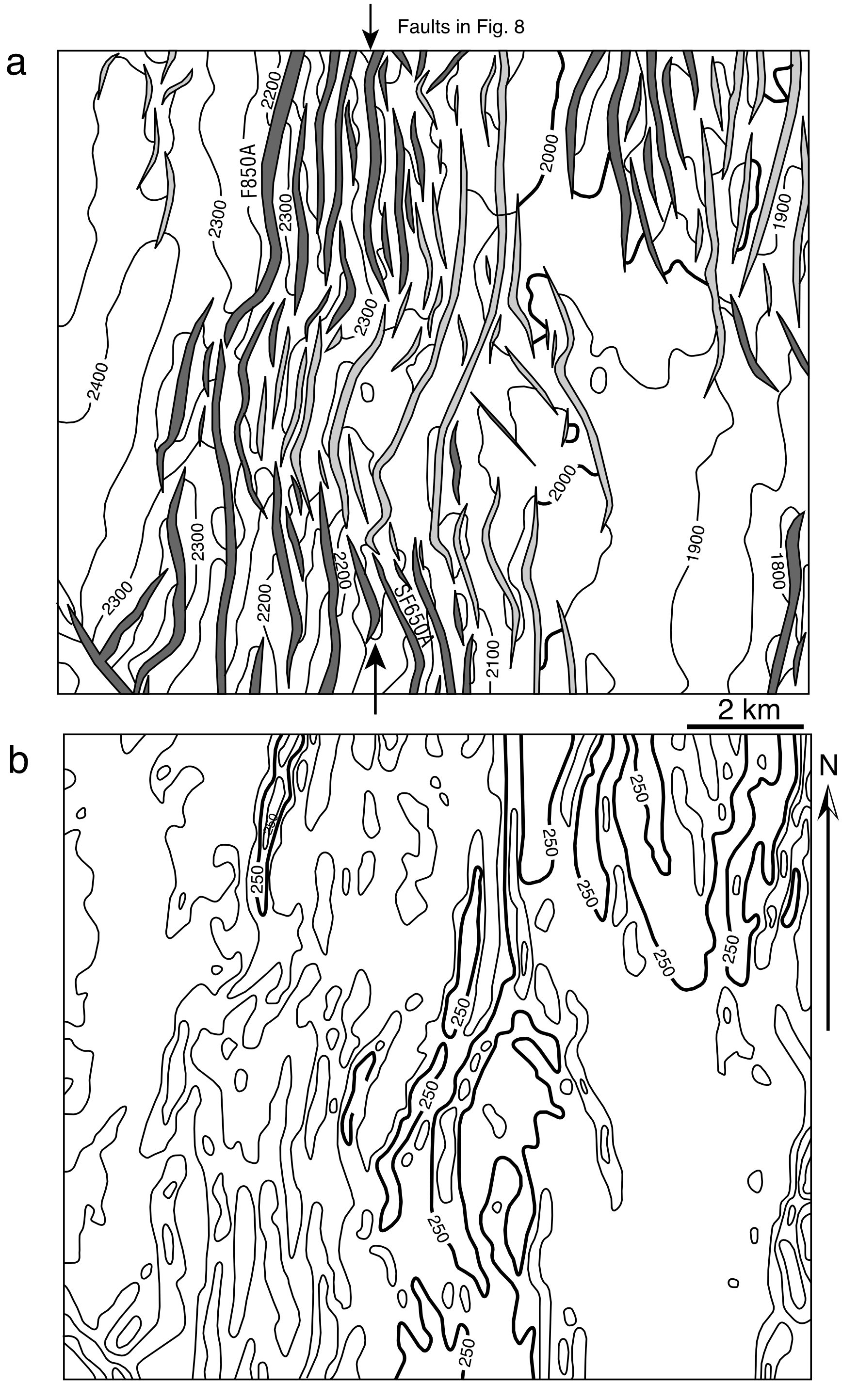

Fig. 7. Time-structure for top Sequence 3 (a) and isochron (b) maps for Sequence 3. See Fig. 3 for location. East dipping faults are black, west dipping faults are grey. Contours in milliseconds.

dominant fault. However a few examples of cross-cutting fault relationships were identified (Fig. 4).

The syn-rift section has a half graben geometry that thickens westwards (Fig. 2). Two faults dominate in the area. The largest fault is SF890M (Fig. 5). On the top basement horizon, and on the isochron map for Sequence 1 two displacement maxima occur along this fault (Fig. 5). At the central displacement minima there is a concentration of west-dipping secondary faults, which, in map view, form a vee-shaped zone up to fault SF890M. Faults F495A and F094H display a synthetic transfer zone geometry.

The structure map at the top of Sequence 1 and the isochron map for Sequence 2 show the displacement maxima on fault SF890M lies at the central part of the

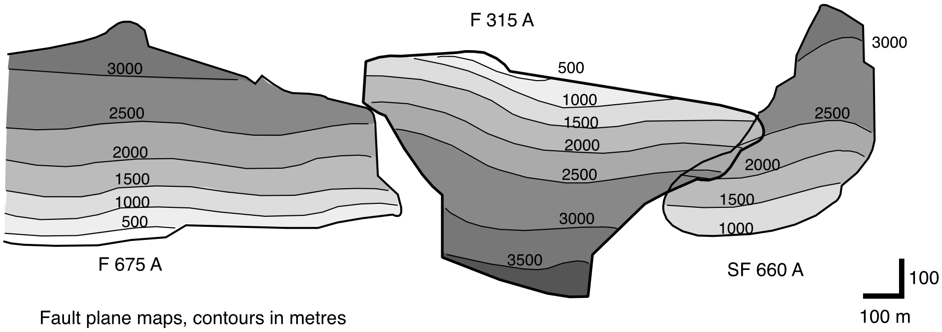

Fig. 8. Structure contour maps for faults SF660A, F315A and F675A, passing across the graben shift, illustrating only slightly overlapping fault geometries in three dimensions. See Fig. 7 for location.

fault (Fig. 6). The two displacement maxima present within Sequence 1 are no longer apparent. The graben shift geometry between the secondary faults is well developed, with many of the fault tips at the dip province boundary curving into NW–SE or NE–SW trending zones. Maps from higher structural levels (Fig. 7) show the graben shift pattern in minor faults; the major SF890M fault is absent (it lies west of the area covered by the seismic survey).

In the Pattani Basin many faults traverse pre-rift basement, the syn-rift and the post-rift section. However, there are also numerous examples of faults confined to either the pre-rift basement and syn-rift sequences, or the post-rift and syn-rift sections but not the basement. In some places unpublished seismic reflection data show that entire conjugate fault systems die out within the post and syn-rift sequences and not a single fault penetrates basement. These data clearly show that the conjugate fault systems nucleate within the post-rift sequence and propagate downwards as well as laterally and upwards. Evidence for nucleation of the conjugate faults in the post-rift section in the Funan Field area is found in fault-displacement patterns, where fault displacement maxima lie in the post-rift section, as discussed below.

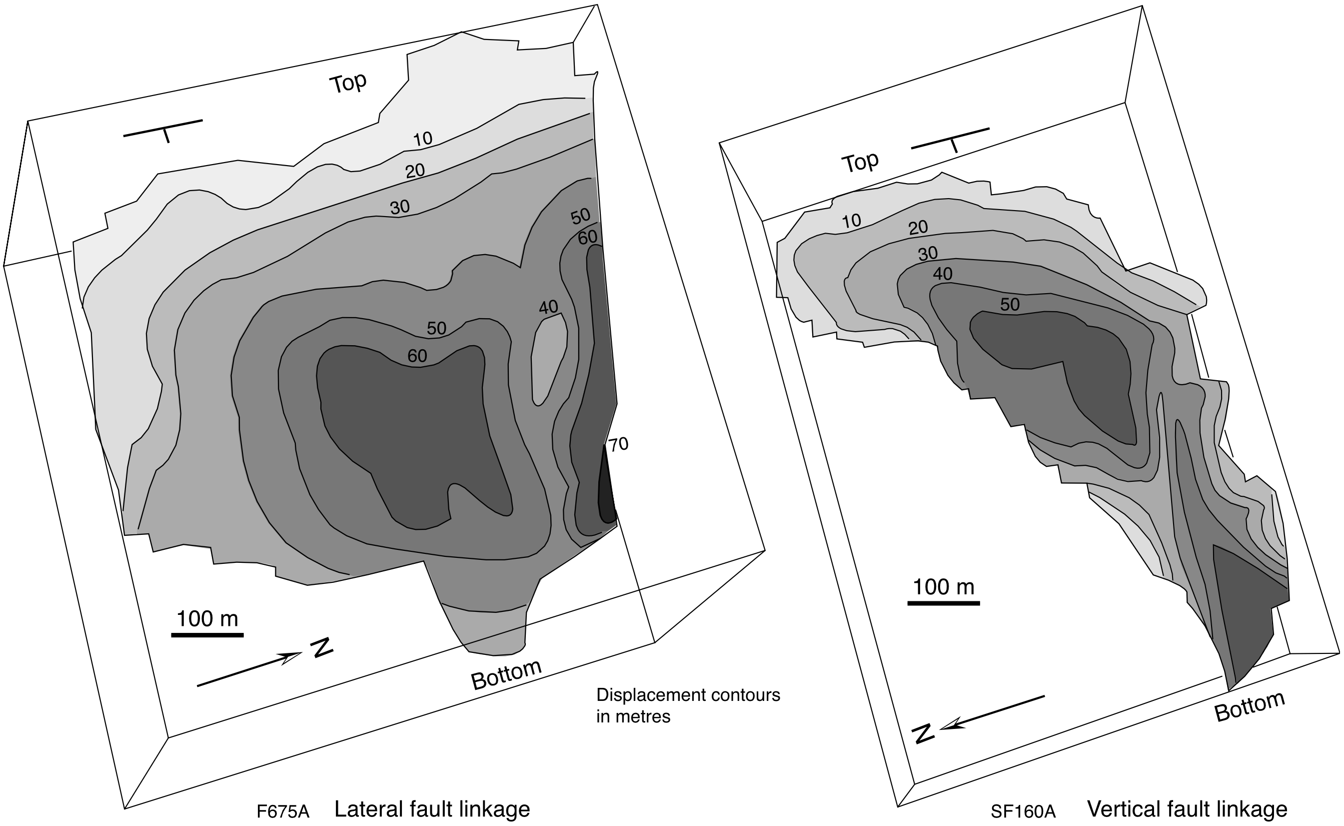

Fig. 9. Examples of fault displacement contours. F675A illustrates lateral fault linkage; SF160A is a west-dipping fault from within the graben shift zone and exhibits vertical linkage of two displacement maxima (see Fig. 7 for location).

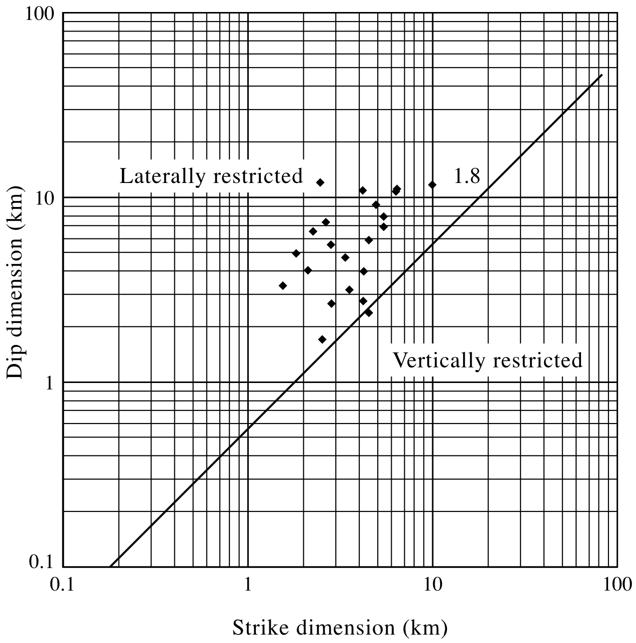

Fig. 10. Graph of fault dimensions (maximum dip length against maximum strike length) for the Funan area. Following Nicol et al. (1996) these data suggest most faults in the Funan area are laterally restricted. The line that corresponds with a strike length to dip length ratio of 1.8 represents the idealised isolated fault ratio defined by Nicol et al. (1996).

Neighbouring faults of opposite dip involved in the graben shift were mapped and their displacement contours calculated using FAPS software (e.g. Needham et al., 1996). In map view adjacent faults of opposite dip display either colinear or slightly overlapping geometries. Contours of the faults show a similar pattern; fault strike length increases upwards (Fig. 8). Displacement of transfer between immediately neighbouring faults does not appear to be significant due to the small amount of overlap for the displacement gradients. Instead transfer must occur between faults of opposite dip within the conjugate fault system that are further away, and have a greater overlap.

Displacement on fault zones forming conjugate fault sets was determined by the vertical offset of mapped horizons on the 3D seismic reflection data (Needham et al., 1996). Some faults display a central displacement maxima. For some faults displacement decreases in all directions (including downwards) away from the centre, other faults have a displacement maxima that increases down to basement. Commonly, more than one region of maximum displacement was found on the fault traces, suggesting the faults formed by amalgamation of two initially separate faults (Fig. 9). In most examples where two displacement maxima are present, they overlie each other suggesting that a fault deep in the section (formed during Sequence 1 time) linked with a later fault, which formed higher in the section. Other faults show evidence for lateral linkage of two horizontally separate faults (Fig. 9); note the loss of displacement downwards on fault F675A.

Unrestricted faults developing in isolation are typically thought to develop elliptical fault shapes and displacement profiles, where the long axis of the ellipse is horizontal (Nicol et al., 1996). Nicol et al. (1996) suggest that the ideal unrestricted fault geometry has a width:height aspect ratio of about 1.8. When a propagating fault reacts to adjacent faults or changes in material behaviour within the rock volume the fault shape will become modified from the ideal unrestricted geometry (Nicol et al., 1996). The result is a restricted fault geometry:aspect ratio for laterally restricted faults typically range from 0.5 to 1.8 and for vertically restricted faults between 1.8 and 8.4 (Nicol et al., 1996). For 21 faults measured in this study the aspect ratios were dominantly those of laterally restricted faults with aspect ratios as low as 0.5 (Fig. 10). However, the problem with using the term laterally restricted is that it implies the fault shape is entirely controlled by the fault propagating faster vertically than it did laterally. For the faults in this study it has also been demonstrated that some of the ‘laterally restricted’ minor west-dipping faults have developed by joining older, deeper faults formed during Sequence 1 with overlying younger faults (Fig. 9), the latter having propagated downwards from a nucleation point in the Middle Miocene section. Consequently for some faults at least part of the large height-to-width ratio could be attributed to up dip fault linkage, not to lateral restriction. The growth of west-dipping faults within a domain of east-dipping faults does, however, suggest that lateral propagation of the west-dipping faults was restricted by the presence of east-dipping faults. Hence two factors have combined to give the laterally restricted geometry.

Wells in the Pattani basin that penetrate shales within Sequence 3 commonly encounter significantly overpressured conditions. Few wells penetrate more than a few hundred metres into the syn-rift sequences; some that do show a return to a hydrostatic pore fluid pressure gradient. The presence of extensive overpressured conditions in Sequence 3 coincides with the nucleation region of conjugate normal faults. Given the impact overpressured fluids have on reducing effective stress, it seems likely that the nucleation of conjugate faults in Sequence 3 is related to the presence of overpressure.

4. Basement fabrics

One possible origin for the graben shift geometry is the influence of pre-existing fabrics in pre-rift ‘basement’ transferred to the conjuage fault system via the syn-rift fault geometry. Consequently, it is necessary to review what kind of ‘basement’ fabrics are likely to exist under the Pattani basin.

Gneissic basement occurs as scattered outcrops around the Gulf of Thailand (Suensilpong et al., 1982). The gneisses may contain inherited Precambrian minerals; however, the last amphibolite overprint was around

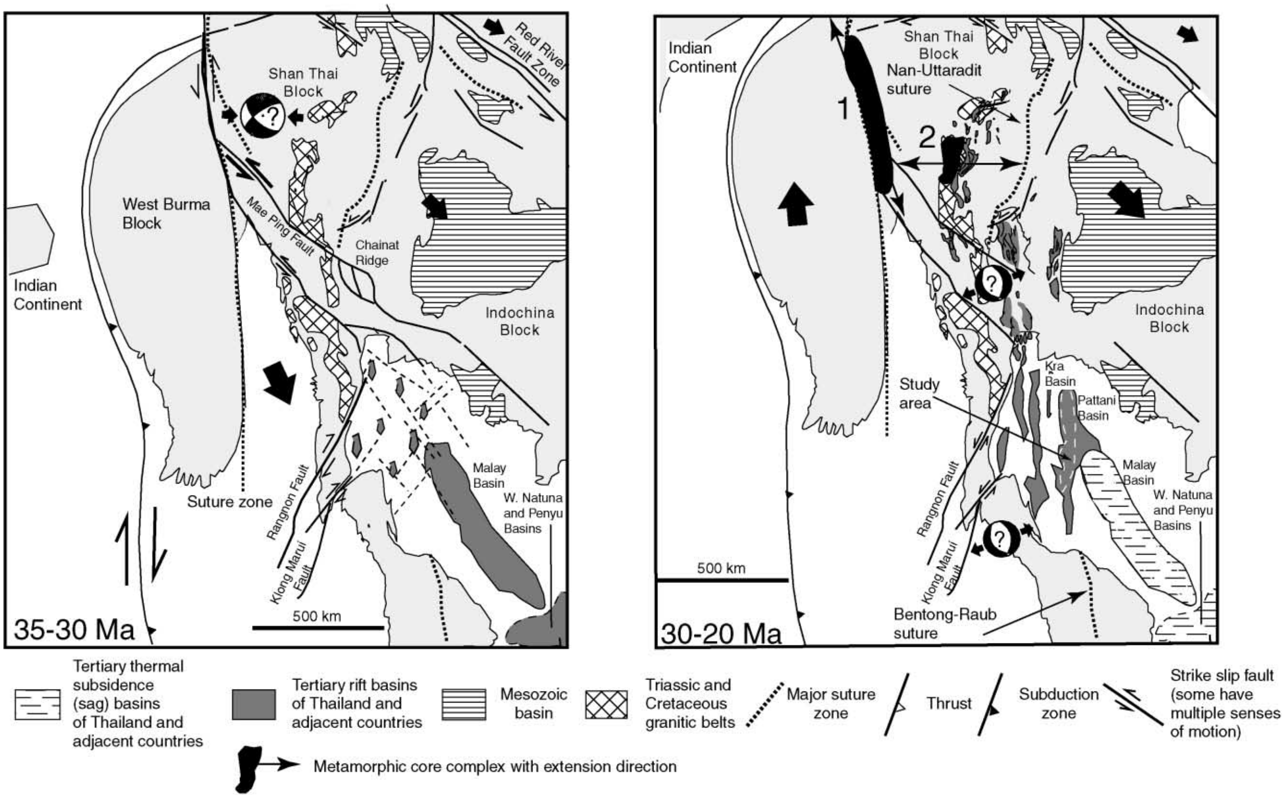

Fig. 11. Geological evolution of SE Asia during the Oligocene and Early Miocene. Map based on the plate reconstructions of Lee and Lawver (1995) and tectonic maps of western Southeast Asia, modified from Packham (1996), Leloup et al. (1995) and Morley (2001). Metamorphic core complex information: (1) Mogok gneiss belt, from Mitchell (1993) and Bertrand et al. (1999); (2) Doi Inthanon and Doi Suthep metamorphic core complexes from Dunning et al. (1995) and Rhodes et al. (1997).

200 Ma (Ahrendt et al., 1997). In southern Thailand zircons dated at 1500–1700 Ma extracted from plutons point to a Precambrian source underlying the peninsula (Liew and Page, 1986).

A number of Paleozoic collisions have imposed important fabrics in the pre-Tertiary basement; they include predominantly N–S to NNW–SSE striking outcrops of highly folded and foliated greenschist grade metasediments of Lower Paleozoic age (Jones 1973; Bunopas 1981). The Nan River Suture Zone in northern Thailand (Bunopas, 1981; Mitchell, 1981; Hahn, 1985; Barr and Macdonald, 1987; Fig. 11) is a major Permo–Triassic suture zone, which may extend into the Bentong–Raub Suture Zone in Peninsula Malaysia (Fig. 11). The Pattani Basin may lie along this suture. However, the extrapolation and linkage of the two suture zones remains hypothetical.

The Indosinian orogeny (250–230 Ma) created dominantly N–S trending fabrics throughout onshore Thailand, which can be projected into the Gulf of Thailand (Cooper et al., 1989). Lying nearly perpendicular to the regional late Tertiary extension direction this fabric has been extensively reactivated by the onshore and offshore Tertiary rift basins. Cretaceous granites that flank and source the sediments of the Pattani Basin have also followed the N–S trend (e.g. Lockhart et al., 1997).

Collision of the West Burma Plate against Eurasia resulted in the Phuket–Mandalay fold belt, associated with S-type granites dated at 70–78 Ma (tin granite belt; Beckinsale et al., 1979). Subsequently the passage of India past the West Burma block resulted in an Eocene orogenic event in Myanmar (Mitchell, 1993). These collisions may have produced motion on some of the major NE–SW and NW–SE trending strike-slip faults in the region (e.g. Polachan and Sattayarak, 1989; Morley 2001). Consequently, there may be some strike-slip related brittle fabrics in the Pattani Basin associated with the Three Pagodas Fault (NW–SE) and the Ranong and Klong–Marui Faults (NE–SW) (Fig. 11).

The Mae Ping fault zone at Lan Sang national park provides the most details about the timing of strike-slip deformation and how basement fabrics are developed. At Lan Sang rocks display NW–SE striking, steeply dipping foliations, with left-lateral ductile shear indicators in ultramylonites over a width of several kilometres (Lacassin et al., 1993). Left lateral deformation along the Mae Ping fault zone ended around 30 Ma (Lacassin et al., 1997). Such fabrics, if present in the Gulf of Thailand, are substantial enough to exert an influence on later fault trends. The termination of left lateral deformation in the Late Oligocene indicates that strike-slip faulting ended prior to significant

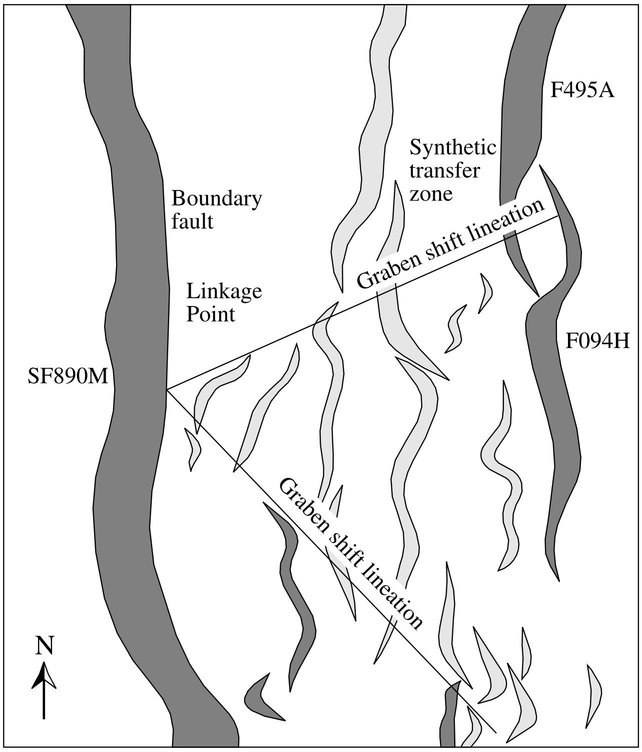

Fig. 12. Indications at the Sequence 1 level that the fault pattern (itself influenced by basement fabrics) later influenced the graben shift pattern. East dipping faults are black, west dipping faults are grey.

rift basin development in the Gulf of Thailand (Fig. 11). Subsequent right lateral motion contemporaneous with rifting has been proposed by Polachan et al. (1991).

The Klong Mariu and Ragnon Faults strike NE–SW and cut through the Isthmus of Kra, crossing from the Gulf of Thailand to the Andaman Sea (Figs. 1 and 11). In plate reconstructions these faults are utilised to accommodate extensional widening of the Gulf of Thailand in the middle-late Tertiary, and they help accommodate counter-clockwise rotation of Peninsula Malaysia with respect to Thailand and Myanmar, as indicated by paleomagnetic studies (Fuller et al., 1991; Lee and Lawver 1995; Hall 1996). The early displacement history (Eocene–Oligocene?) of the two faults was probably right lateral, which is consistent (for conjugate fault sets) with left lateral displacement on the major NW–SE trending Mae Ping and Three Pagodas Faults. In the Early Miocene displacement on the Klong Mariu and Ragnon Faults is suggested to have become left lateral (Polachan et al., 1991; Lee and Lawver 1995). The amount of displacement is uncertain; matching offsets of Mesozoic rocks across the Klong Mariu Fault from the regional geological map (Suensilpong et al., 1982) indicates right lateral displacement of up to 100 km. How much of the original right-lateral offset has been reduced by subsequent left lateral motion is difficult to quantify. However, since it is difficult to identify any significant offset of sedimentary basins by the fault, left lateral motion was probably minor.

5. Discussion

The possible origins of the graben shift geometry include the following:

1. They are random features confined to the post-rift section.
2. They are related (in some way) to active strike-slip faulting.
3. They are related to some kind of passive pre-existing basement fabric.

The Sequence1 isochron and structure maps provide important clues about the development of the graben shift geometries. The boundary fault SF890M lies west of the graben shift, and it is not offset or cut by the projected NE–SW and NW–SE transfer zone boundaries of the graben shift, hence there is no indication of active strike-slip trends in the area. This is typical for the entire Pattani Basin (Watcharanantakul and Morley, 2000). Normal faults display bends or entire segments that strike in a NW or NE direction (e.g. Lockhart et al., 1997; Watcharanantakul and Morley, 2000), but there is no line of continuous offset across the Pattani Basin that indicates active strike-slip tectonics as proposed by Polachan et al. (1991). Instead the Paleogene strike-slip fault activity appears to have been replaced by extension in the Late Oligocene, and any influence by the strike-slip faults is as a passive fabric (Watcharanantakul and Morley, 2000; Fig. 11).

The slightly overlapping nature of faults in the transfer zones also indicates a non-strike-slip origin. The projected graben shift boundaries show the following characteristics (Fig. 12): (1) they converge on the area of low displacement in the centre of SF890M, and (2) they define the limit of the minor antithetic faults active during Sequence 1. The NE–SW trending boundary runs into the relay ramp between faults F094H and F495A. There is also a tendency for the fault tips at the transfer zone to curve into alignment with the transfer zone trends. These observations suggest that there is a NE–SW trending boundary, caused by a relatively strong zone in the basement, which inhibited fault propagation during Sequence 1 times. Probably the same applies to the southern NW–SE trending boundary. The antithetic (west dipping) minor faults may have developed to accommodate the drop in extension along fault SF890M as it died out towards the central region. The antithetic faults are also limited by the inferred strength barriers.

The exact influence of the pre-existing fabric anomalies unfortunately cannot be determined. Important fabrics could be related to older (Mesozoic or early Tertiary) strike-slip trends (for example Y, R′ and P shear trends associated with a NW–SW striking sinistral fault, or a NE–SW striking dextral fault (Fig. 11). Alternatively, it could be the effects of older Mesozoic, Palaeozoic or Precambrian structural fabrics, juxtaposition of different lithologies across faults, or igneous intrusions related to events discussed in the

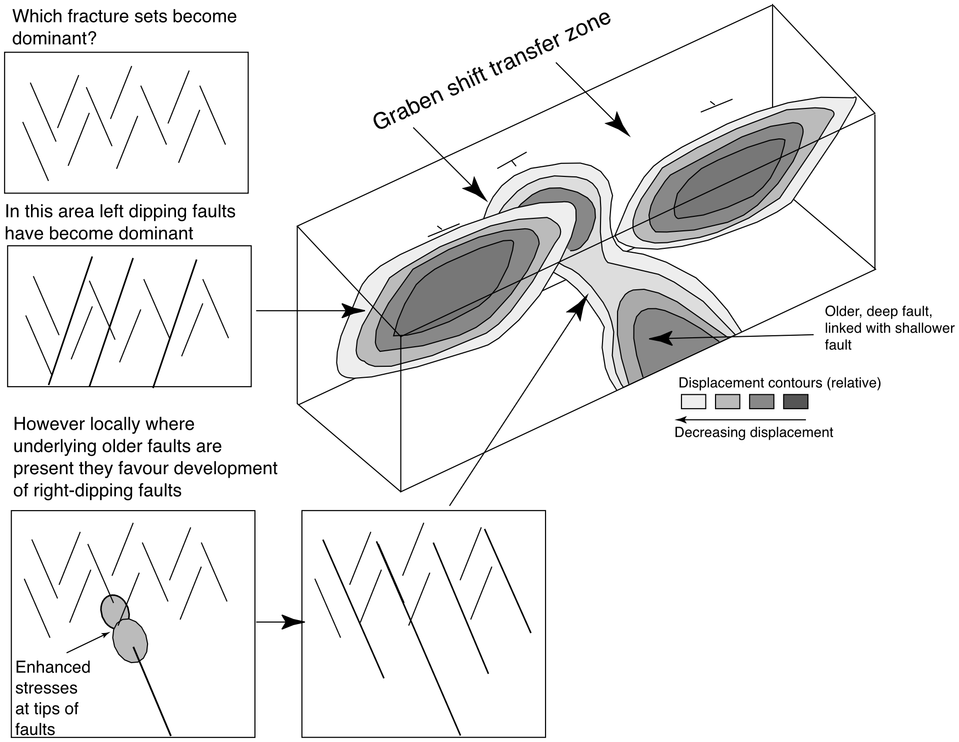

Fig. 13. Schematic diagram illustrating how the graben shift geometry may have evolved. Left dipping faults tend to become dominant as strain increases on a set of initially low displacement conjugate fractures. However, where a deeper right dipping fault exists it links with a higher right-dipping fracture, which subsequently promotes the development of more synthetic fault sets. Stress fields around two vertically in line or en échelon faults will interact and promote fault linkage (following Cowie, 1998).

previous section. However, given the strong fabric developed in association with the Mae Ping fault zone, and the common NW–SE to NNW–SSE trends followed by normal faults (e.g. Lockhart et al., 1997; Watcharanantakul and Morley, 2000) influence by passive strike-slip fault trends seems very likely.

During Sequence 2, fault SF890M continued to develop and the original linkage geometry was eradicated. However, the influence of the Sequence 1 geometry on the secondary faults was inherited by Sequence 2 and the overlying sequences. Typically in rifts secondary faults tend to lie synthetic to boundary faults (e.g. Morley, 1995), so with the development of SF890M during Sequence 2 the secondary faults close to the fault also dipped to the east. However, these east-dipping minor faults had to adapt to the previously established anomalous area of west-dipping secondary faults. Hence the graben shift geometry developed. This pattern apparently exerted an influence even on faults that nucleated higher in the section during the Middle and Upper Miocene and gave rise to the two vertically stacked displacement maxima seen on several west-dipping minor faults (Fig. 9; SF160A).

Price and Cosgrove (1990, p. 207) noted that the occurrence of conjugate fault sets where both orientations are of similar frequency, dimensions and displacement is rare. Instead groups of faults of similar dip tend to become dominant, with the other conjugate set either just a minor component, or not even present. They attributed fault group dips to the orientation of the first fault of significant size that develops. That first fault will cause a significant reduction in the differential stress in the surrounding rock volume. The geometry of the zone of decreased differential stress tends to inhibit conjugate fault sets from forming, and promotes synthetic fault development (Price and Cosgrove, 1990). This explanation for conjugate fault set development seems appropriate for the Funan Field area (Fig. 13).

In the Pattani Basin as a whole the total length of major east-dipping syn-rift faults mapped from seismic reflection data is 2.3 times greater than west-dipping faults. This pattern is reflected in the conjugate faults sets, where the area covered by east-dipping conjugate fault provinces is about 50% larger than west-dipping fault provinces. There is, in general, a good correspondence between the location of major east-dipping faults, and overlying east-dipping fault provinces. The younger conjugate faults sets tend to follow the trends either by reactivating the deeper boundary faults or by forming synthetic sets to the deeper boundary fault. In the Funan area the conjugate faults closest to the boundary fault (SF890M) are synthetic to it (Fig. 4), suggesting that stress distribution around the pre-existing fault influenced later fracture orientation, as described above and in Price and Cosgrove (1990). The same pattern is repeated for the Gomin conjugate fault system in Fig. 4a and b. The conjugate fault system exists where the syn-rift faults F094H and F495A are present. When the syn-rift faults die out to the south (Fig. 4c) the conjugate fault system also dies out.

The graben shift in the Funan area appears to represent a perturbation of the stress field that promoted the development of west-dipping faults, which can be explained by pre-existing syn-rift faults. The graben shift occurs in an area of anomalous syn-rift fault geometry, where secondary, west-dipping syn-rift faults antithetic to the main fault (SF890M) are developed (Fig. 5). These minor syn-rift faults developed in the region where the boundary fault (SF890M) decreased in displacement in Sequence 1 times (Figs. 5 and 12) and appear to be limited by NE–SW and NW–SE trending lineaments probably related to pre-existing fabrics.

Cowie (1998) presented numerical models of fault growth showing certain fault configurations in map view that enhanced or inhibited fault growth as a result of being in areas of stress shadow or stress superimposition. In particular high stresses at en échelon fault tips promoted fault propagation and linkage. While Cowie (1998) was concerned with fault development in map view the same effects must occur naturally in three dimensions. The linkage of younger and older faults antithetic to fault SF890M mentioned above and illustrated in Fig. 9 would appear to represent the same effects in a vertical sense (Fig. 13).

6. Conclusions

Arrays of slightly overlapping convergent transfer zones, locally called graben shifts, between sets of opposite-dipping conjugate minor normal faults are very common in the Pattani Basin. One example of a graben shift from the Funan Field shows the following fault geometries and displacement characteristics:

1. The graben shifts trend NE–SW and NW–SE at a high angle to the N–S striking normal faults.
2. Faults at the transfer zone only slightly overlap with their neighbours, and the strike-length of the fault zones tends to increase upwards. Displacement transfer must occur between more widely separated faults in the transfer zone because the areas of overlap between neighbouring faults of opposite dip is so small and displacement gradients are correspondingly high.
3. Fault displacement diagrams for the anomalous zone of west dipping faults forming the graben shift incursion into the zone of east-dipping faults show vertical linkage of two initially separate faults as suggested by two displacement maxima. One displacement maximum formed during Sequence 1, the other during Sequence 3 or later. Sequence 1 west dipping faults were confined to the present day area of the graben shift. Nucleation of the faults in Sequence 3 is probably related to overpressured pore fluids.
4. During Sequence 1 times the line of the NE–SW boundary to the graben shift coincided with fault segment linkage geometries in both the largest and second largest faults in the study area, as well as the termination of minor faults. The minor fault tips tend to curve into the boundary line. All these data suggest there was a passive linear strength barrier related to pre-existing fabrics in basement that strongly influenced fault propagation geometries. The pre-existing fabric could be related to inactive Paleogene strike-slip faults.
5. ‘Laterally restricted’ geometries, particularly in the west-dipping conjugate fault sets, are a result of vertical linkage of faults and inhibition of west-dipping fault propagation laterally into fields of east-dipping faults.
6. There is no indication of active strike-slip faulting affecting the graben shift geometry. Instead two stages of inherited passive fabrics are the cause of the geometry. Pre-existing fabrics influenced Sequence 1 faults. Then the Sequence 1 fault pattern later influenced the Sequence 3 fault pattern. Hence indirectly pre-existing basement trends were imposed on the conjugate fault sets.
7. Normal faults deeper in the section exerted an influence on the development of later faults, higher in the section. Probably the build up of stresses at the tips of older faults in the syn-rift section, and younger faults propagating from higher in the section promoted vertical linkage on faults with an en échelon or in line alignment.

Acknowledgements

We would like to thank Unocal Thailand for providing the data and permission to publish and Landmark for providing the 3D interpretation software to the University Brunei Darussalam. A. Nicol and C. Elders are thanked for helpful, constructive reviews that improved the manuscript. Badleys are thanked for providing the FAPS software and technical support under an academic agreement.

References

Ahrendt, H., Hansen, B.T., Lumjuan, A., Mickein, A., Wemmer, K., 1997. Tectonometamorphic evolution of NW-Thailand deduced from U/Pb-Sm/Nd- and K/Ar-isotope investigations. The International Conference on Stratigraphy and Tectonic Evolution of Southeast Asia and the South Pacific, Bangkok, Thailand, pp. 314–319.

Barr, M.S., Macdonald, A.S., 1987. Nan River Suture Zone, Northern Thailand. Geology 15, 907–910.

Beckinsale, R.D., Suensilpong, S., Nakapadungrat, S., Walsh, J.N., Cobbing, E.J., Ridd, M.F., 1979. Geochronology and geochemistry of granite magmatism in Thailand in relation to a plate tectonic model. Journal of the Geological Society, London 136, 529–540.

Bertrand, G., Thein, M., Myint, O., Maw, W., Lwin, S., Rangin, C., Maluski, H., Han, T.A., 1999. Cenozoic metamorphism along the

Shan scarp (Myanmar): Evidence for ductile shear along the Sagaing fault or the northward migration of the eastern Himalayan syntaxis? Geophysical Research Letters 26, 915–918.

Bunopas, S, 1981. Palaeogeographic history of western Thailand and adjacent parts of S.E. Asia; a plate tectonic interpretation. Geological Survey Paper 5, Mineral Resources, Thailand, 81pp.

Bustin, R.M., Chonchawalit, A., 1995. Formation and tectonic evolution of the Pattani Basin, Gulf of Thailand. International Geology Review 37, 866–892.

Cooper, M.A., Herbert, R., Hill, G.S., 1989. The structural evolution of Triassic intermontaine basins in northeastern Thailand. International Symposium on Intermontaine Basins: Geology & Resources, Chiang Mai, Thailand, 12pp.

Cowie, P.A., 1998. A healing-reloading feedback control on the growth rate of seismogenic faults. Journal of Structural Geology 20, 1075–1087.

Dunning, G.R., Macdonald, A.S., Barr, S.M., 1995. Zircon and monazite U–Pb dating of the Doi Inthanon core complex, northern Thailand: implictions for extension within the Indosinian Orogen. Tectonophysics 251, 197–213.

Fuller, M., Haston, R., Jin-Lu, L., Richter, B., Schmidtke, E., Almasco, J., 1991. Tertiary paleomagnetism of the regions around the S. China Sea. Journal of Southeast Asian Earth Science 6, 161–184.

Jardine, E., 1997. Dual petroleum systems governing the prolific Pattani Basin, offshore Thailand. Petroleum systems of S.E. Asia and Australasia Conference, Jakarta, May 21–23, 1997, pp. 351–363.

Jones, C.R., 1973. Lower Paleozoic. In: Gobbett, D.J., Hutchison, C.S. (Eds.). Geology of the Malay Peninsula. John Wiley-Interscience, New York, pp. 25–60.

Lacassin, R., Leloup, P.H., Tapponnier, P., 1993. Bounds on strain in large Tertiary shear zones of SE Asia from boudinage restoration. Journal of Structural Geology 15, 677–692.

Lacassin, R., Hinthong, C., Siribhakdi, K., Chauviroj, S., Charoenravat, A., Maluski, H., Leloup, P.H., Tapponier, P., 1997. Tertiary diachronic extrusion and deformation of western Indochina: structure and ^{40}Ar/^{39}Ar evidence from NW Thailand. Journal of Geophysical Research 102 (B5), 10013–10037.

Lee, T.-Y., Lawver, L.A., 1995. Cenozoic plate reconstructions of Southeast Asia. Tectonophysics 251, 85–138.

Leloup, P.H., Lasassin, R., Tapponier, P., Scharer, U., Dalai, Z., Xiaohan, L., Liangshang, Z., Shaocheng, J., Trinh, P.T., 1995. The Ailao Shan–Red River shear zone (Yunnan, China), Tertiary transform boundary of Indochina. Tectonophysics 251, 3–84.

Lian, H.M., Bradley, K., 1986. Exploration and development of natural gas, Pattani Basin, Gulf of Thailand. Transactions of the Fourth Circum-Pacific Energy and Mineral Resources Conference, Singapore, pp. 171–181.

Liew, T.C., Page, R.W., 1986. U–Pb zircon dating of granitoid plutons from the west coast province of peninsula Malaysia. Journal of the Geological Society of London 142, 515–526.

Lockhart, B.E., Chinoroje, O., Enomoto, C.B., Hollomon, G.A., 1997. Early Tertiary deposition in the southern Pattani Trough, Gulf of Thailand. In: Dheeradilok, P. (Ed.). Stratigraphy and Tectonic Evolution of Southeast Asia and the South Pacific. Department of Mineral Resources, Thailand, pp. 476–489.

Hahn, L., 1985. The Indosinian Orogeny in Thailand and adjacent areas. Memoire Geological Society France 147, 71–82.

Hall, R., 1996. Reconstructing Cenozoic SE Asia. In: Hall, R., Blundell, D.J. (Eds.). Tectonic Evolution of Southeast Asia. Geological Society, London, pp. 203–224. Special Publications 106.

McCabe, R., Harder, S., Cole, J.T., Lumadyo, E., 1993. The use of paleomagnetic studies in understanding the complex Tertiary tectonic history of East and Southeast Asia. Journal of Southeast Asia Earth Sciences 8, 257–268.

Mitchell, A.G.H., 1981. Phanerozoic plate boundaries in mainland S.E. Asia, the Himalayas and Tibet. Geological Society of London 138, 109–122.

Mitchell, A.H.G., 1993. Cretaceous–Cenozoic tectonic events in the Western Myanmar (Burma) Assam Region. Journal of the Geological Society, London 150, 1089–1102.

Morley, C.K., 1995. Developments in the structural geology of rifts over the last decade and their impact on hydrocarbon exploration. In: Lambiase, J.J., Hydrocarbon Habitat in Rift Basins, Geological Society Special Publication, 80, 1–32.

Morley, C.K., 2001. Combined escape tectonics and subduction rollback-back arc extension: a model for the evolution of Tertiary rift basins in Thailand, Malaysia and Laos. Journal of the Geological Society, London 158, 461–471.

Morley, C.K., Sangkumarn, N., Hoon, T.B., Chonglakmani, C., Lambiase, J., 2000. Structural evolution of the Li Basin northern Thailand. Journal of the Geological Society of London 157, 483–492.

Needham, T., Yielding, G., Freeman, B., 1996. Analysis of fault geometry and displacement patterns. In: Buchanan, P.G., Nieuwlands, D.A. (Eds.). Modern Developments in Structural Interpretation, Validation and Modelling. Geological Society of London Special Publication 99, pp. 189–199.

Nicol, A., Watterson, J., Walsh, J., Childs, C., 1996. The shapes, major axis orientations and displacement patterns of fault surfaces. Journal of Structural Geology 18, 235–248.

Oudom-Ugsorn, P., Bunopas, S., Achalabhuti, C., Polachan, S., 1986. Petroleum potential in pre-Tertiary basins of Thailand. ASCOPE, Indonesia 12, 1997.

Packham, G., 1996. Cenozoic SE Asia: reconstructing its aggregation and reorganization. In: Hall, R., Blundell, D.J. (Eds.). Tectonic Evolution of Southeast Asia. Geological Society, London, pp. 123–152. Special Publication 106.

Polachan, S., Sattayarak, N., 1989. Strike-slip tectonics and the development of Tertiary basins in Thailand. International Symposium on Intermontane Basins: Geology and Resources, Chiang Mai, Thailand, pp. 243–253.

Polachan, S., Pradidtan, S., Tongtaow, C., Janmaha, S., Intarawijitr, K., Sangsuwan, C., 1991. Development of Cenozoic basins in Thailand. Marine and Petroleum Geology 8, 84–97.

Pradidtan, S., Dook, R., 1992. Petroleum geology of northern part of the Gulf of Thailand. National Conference on Geological Resources of Thailand: Potential for Future Development, Department of Mineral Resources, Bangkok, Thailand.

Price, N.J., Cosgrove, J.W., 1990. Analysis of Geological Structures. Cambridge University Press, Cambridge, 502pp.

Rhodes, B.P., Blum, J., Devine, T., 1997. Geology of the Doi Suthep metamorphic core complex and adjacent Chiang Mai Basin. The International Conference on Stratigraphy and Tectonic Evolution of Southeast Asia and the South Pacific, Bangkok, Thailand, pp. 305–313.

Suensilpong, S., Nakornsri, N., Dheeradilok, P., Lumjuan, A., Tansathien, W. Vimuktanandana, S., 1982. Geological Map of Thailand. Geological Survey Division, Department of Mineral Resources, Thailand, Scale 1:1,000,000, 2 sheets.

Tapponnier, P., Peltzer, G., Le Dain, A.Y., Armijo, R., Cobbold, P., 1982. Propagating extrusion tectonics in Asia; new insights from simple experiments with plasticine. Geology 10, 611–616.

Tapponnier, P., Peltzer, G., Armijo, R., 1986. On the mechanism of collision between India and Asia. In: Coward, M.P., Ries, A.C. (Eds.). Collision Tectonics. Geological Society, London, pp. 115–157 Special Publications, 19.

Watcharanantakul, R., Morley, C.K., 2000. Syn-rift and post-rift modelling of the Pattani Basin, Thailand: evidence for a ramp-flat detachment. Marine and Petroleum Geology 17, 937–958.